Electronic Supplementary Material (ESI) for Catalysis Science & Technology.
This journal is © The Royal Society of Chemistry 2022

Supplementary Information

Evaluation of the external and internal mass transfer limitations

The external mass transfer limitations were estimated by the Carberry criterion with the equation below:

$$Ca = \frac{r_{v,\,obs}}{a' k_f C_b} < 0.05$$

where $r_{v,\,obs}$ is the observed reaction rate for NO conversion, a' is the a' = Ap/Vp is the specific area, k_f is the mass transfer coefficient (0.15 m/s, from [1]) and C_b is the NO concentration in the gas phase. The value of the Ca number at 150 °C for the maximum observed rate is 0.011, which satisfies the criteria and therefore the absence of external mass transport is confirmed.

The resistance of internal mass transfer inside of the catalyst particles was estimated by the Weisz-Prater criterion[2], as shown in the equation (1)

$$\eta\phi^2 = \frac{r_{v,\,obs} \cdot L^2}{D_{eff} \cdot C_s} < 0.15 \qquad (1)$$

where $r_{v,\,obs}$ is the observed reaction rate for NO conversion, L is the characteristic length of the catalyst particles (we have considered particles of an average radius of 300 μm). D_{eff} is the NO effective diffusivity, which was taken from[3] ($3 \cdot 10^{-6}$ m^2/s) and Cs is the NO surface concentration. The calculated value at 150 °C for the maximum observed rate is 0.056, therefore the reaction is not internal mass-transfer limited.

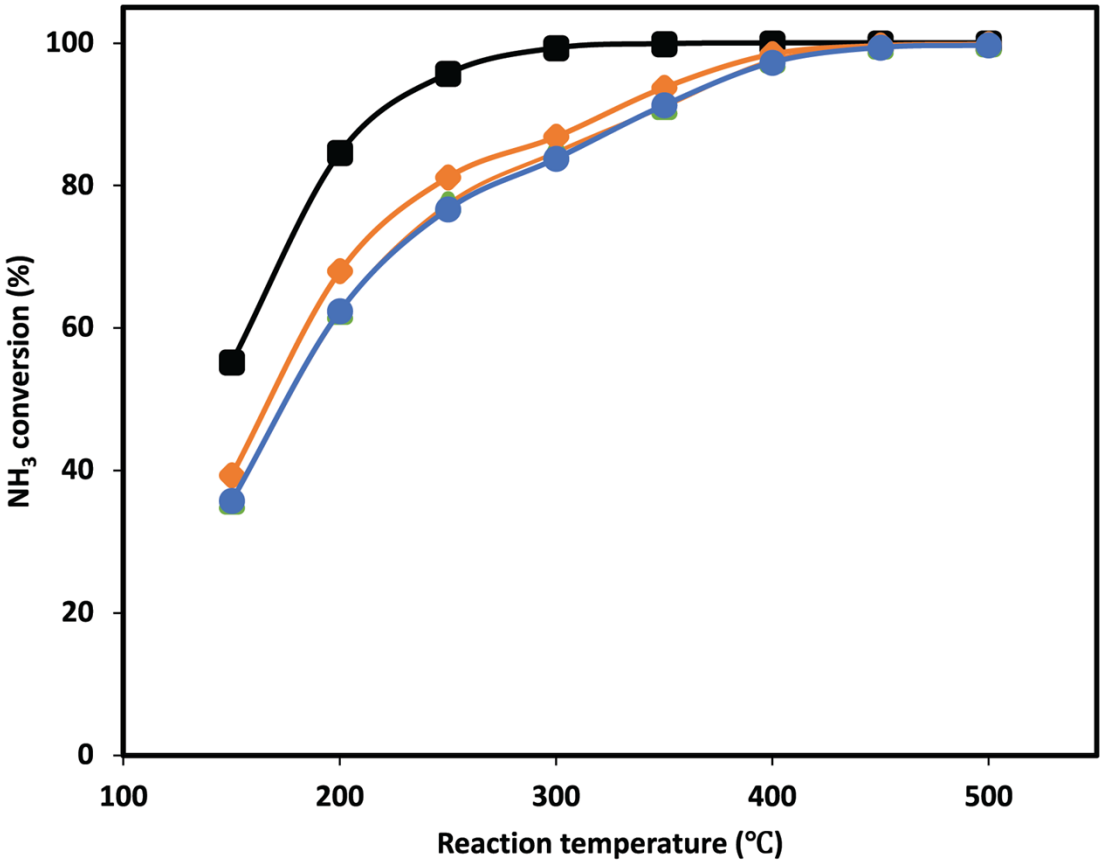

Supplementary Fig 1. NH_3 conversion as a function of the reaction temperature for $Mn_{0.35}Ce_{0.00}Ti_{0.65}$ (black), $Mn_{0.37}Ce_{0.04}Ti_{0.59}$ (orange), $Mn_{0.33}Ce_{0.07}Ti_{0.60}$ (green), $Mn_{0.30}Ce_{0.19}Ti_{0.51}$ (blue).

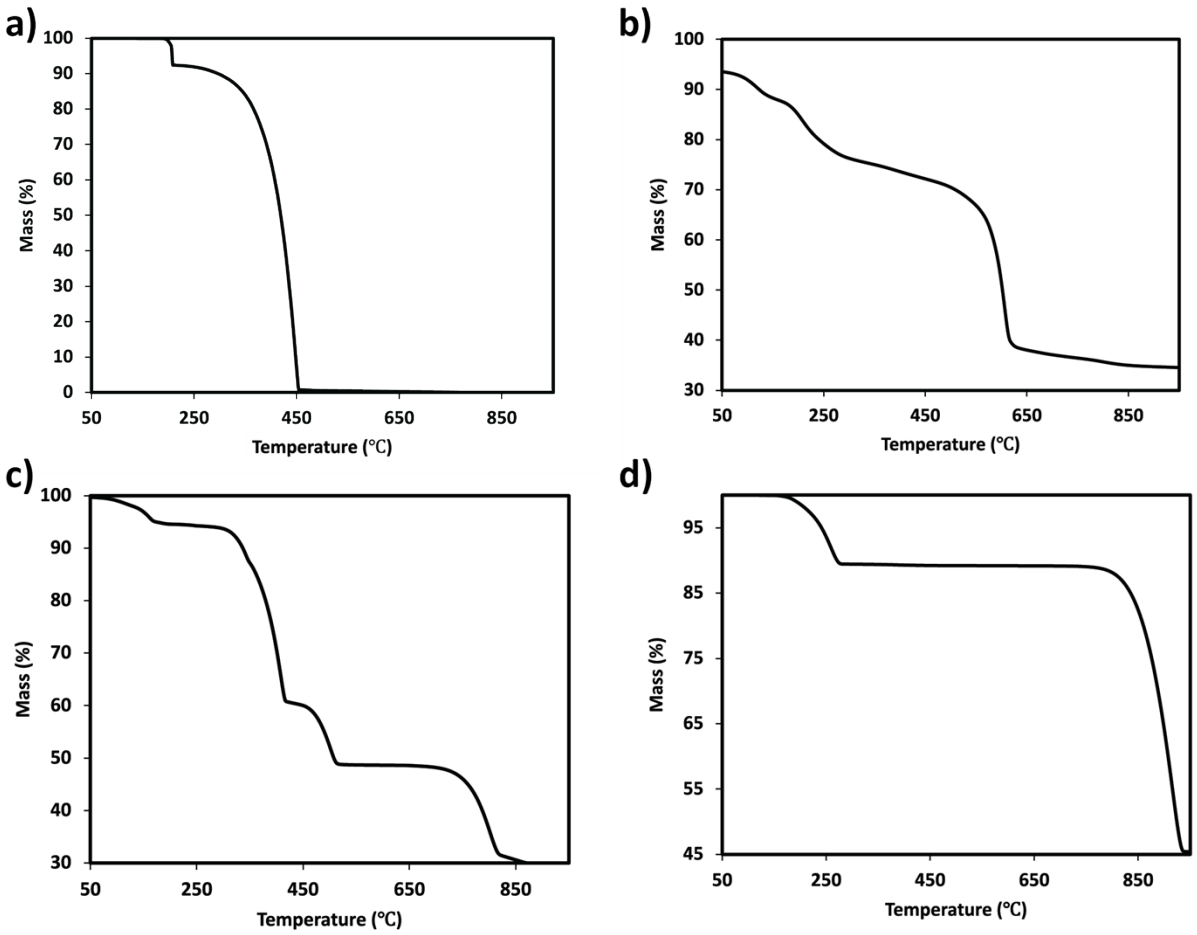

Supplementary Fig 2. TGA analysis of a) ammonium persulfate, b) Ti (IV) oxysulfate, c) Ce (IV) sulfate and d) Mn (II) sulfate.

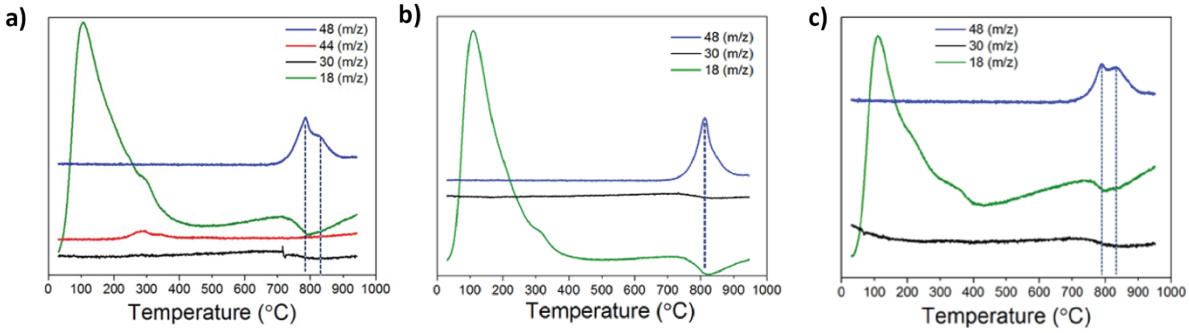

Supplementary Fig 3. Mass spectrometry analysis of the gases coming out of the TGA analysis of the a) $Mn_{0.35}Ce_{0.00}Ti_{0.65}$, b) $Mn_{0.37}Ce_{0.04}Ti_{0.59}$ and c) $Mn_{0.30}Ce_{0.19}Ti_{0.51}$ samples upon NH_3-SCR reaction with SO_2.

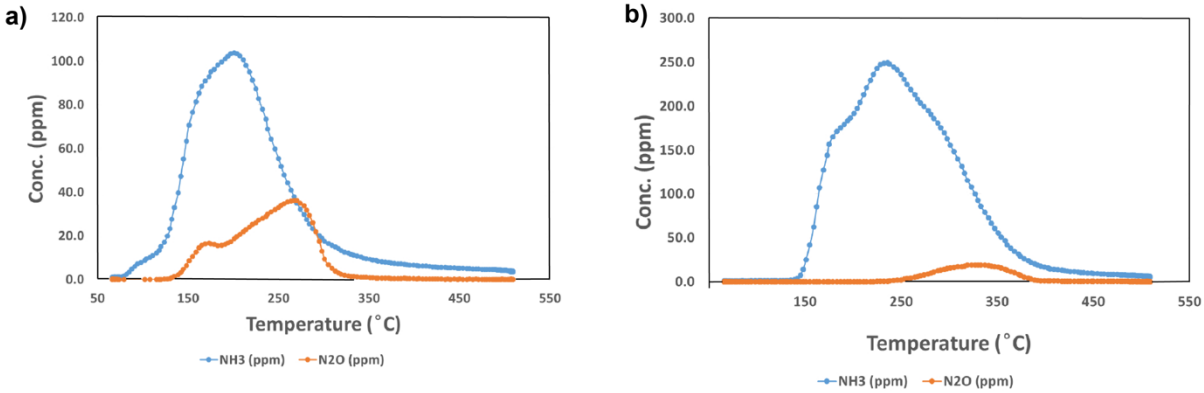

Supplementary Fig 4. Temperature-programmed desorption of NH_3 for the a) $Mn_{0.35}Ce_{0.00}Ti_{0.65}$ sample as fresh and b) upon SO_2 deactivation. The orange line shows the evolution of N_2O, which is coming from the partial oxidation of NH_3 on the catalyst surface.

Supplementary Table 1. Total amount of NH_3 and N_2O release during NH_3-TPD experiments.

Samples	NH_3, (µmol/g)	N_2O, (µmol/g)	Total, (µmol/g)
$Mn_{0.35}Ce_{0.00}Ti_{0.65}$	39.6	12.1	63.7
$Mn_{0.35}Ce_{0.00}Ti_{0.65}$ after SO_2	98.2	4.9	108

XPS analysis and results

To model the Mn($2p_{3/2}$) peaks of the catalysts, pure MnO, Mn_2O_3,MnO_2 and $MnSO_4$ samples were used as reference samples. Manganese(IV) oxide (99.997% - metals basis) was acquired from Alfa Aesar (Fisher US), manganese(III) oxide (99.9% - trace metals basis) was acquired from Sigma Aldrich. Manganese(II) oxide (99.99% - trace metal basis) and manganese(II) sulfate monohydrate (98+%) was acquired from Acros Organics (VWR). The fitting parameters data (FWHM and peak positions) obtained from the peak modelling of the standard samples were used for the calculation of the chemical state of manganese. Mn($2p_{3/2}$) spectra of the reference samples are plotted in Supplementary Fig 4. The fitting parameter data (FWHM and peak position) used for the calculation of the chemical states of manganese in the catalysts can be found in our previous publication[4]

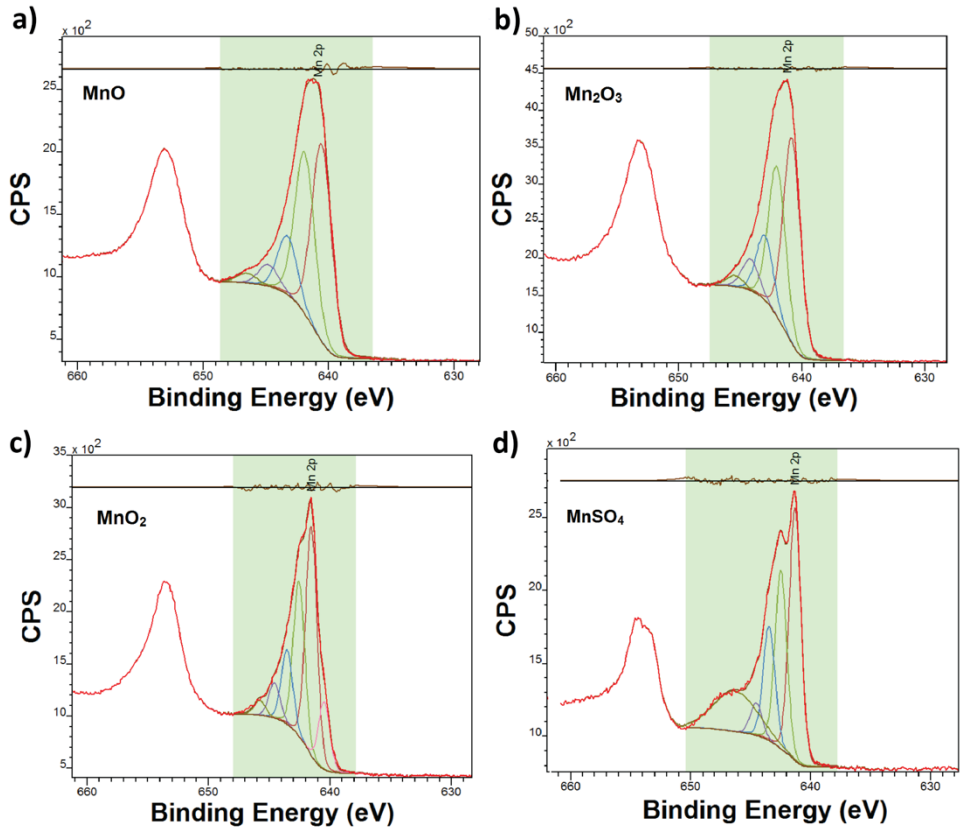

Supplementary Fig 5. Mn 2p spectra of a) MnO, b) Mn_2O_3, c) MnO_2 and d) $MnSO_4$

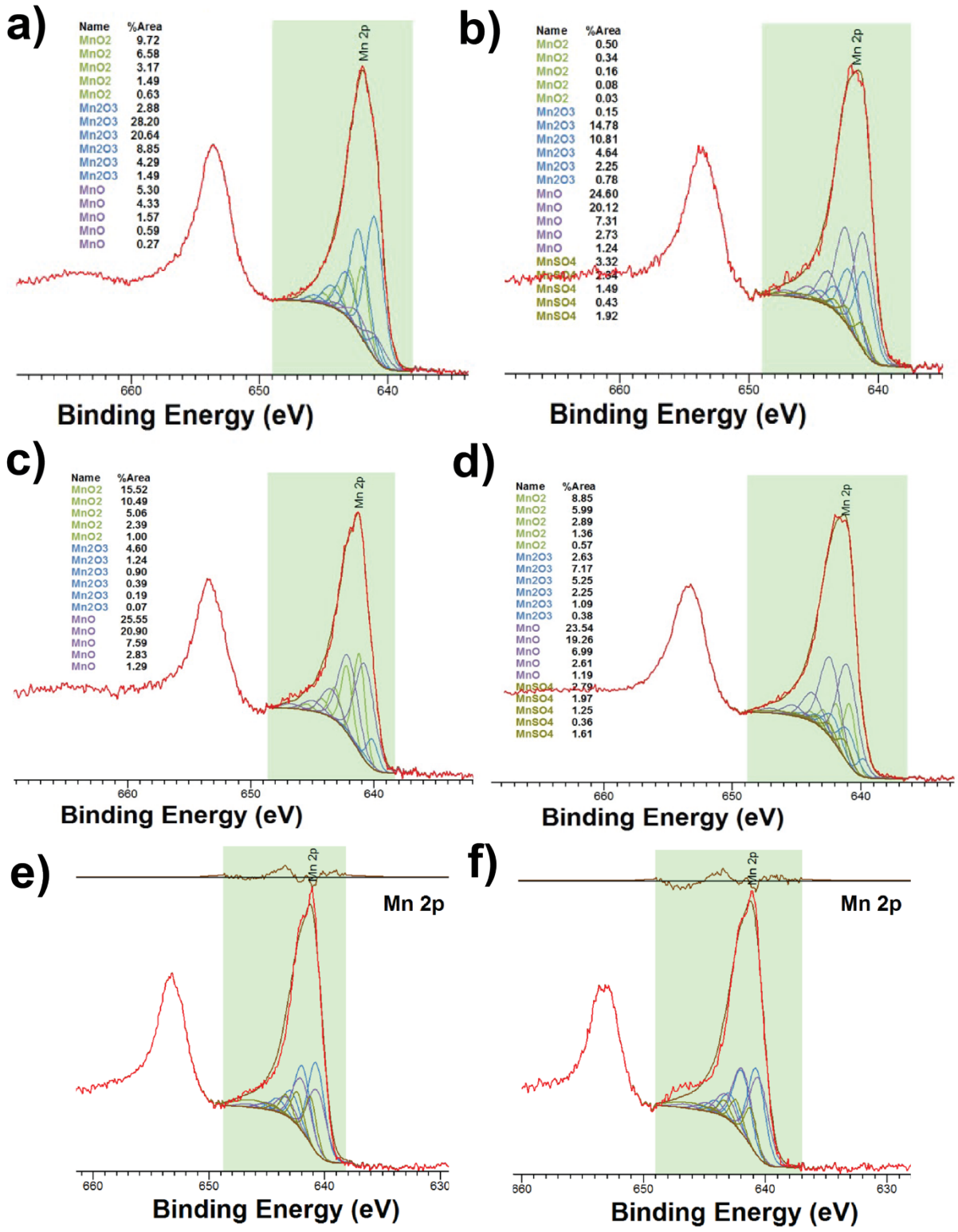

Supplementary Fig 6. Mn 2p spectra of $Mn_{0.35}Ce_{0.00}Ti_{0.65}$, a) fresh and b) after SO_2 deactivation. $Mn_{0.37}Ce_{0.04}Ti_{0.59}$ c) fresh and d) after SO_2 deactivation. $Mn_{0.30}Ce_{0.19}Ti_{0.51}$ sample as e) fresh and f) after SO_2 deactivation.

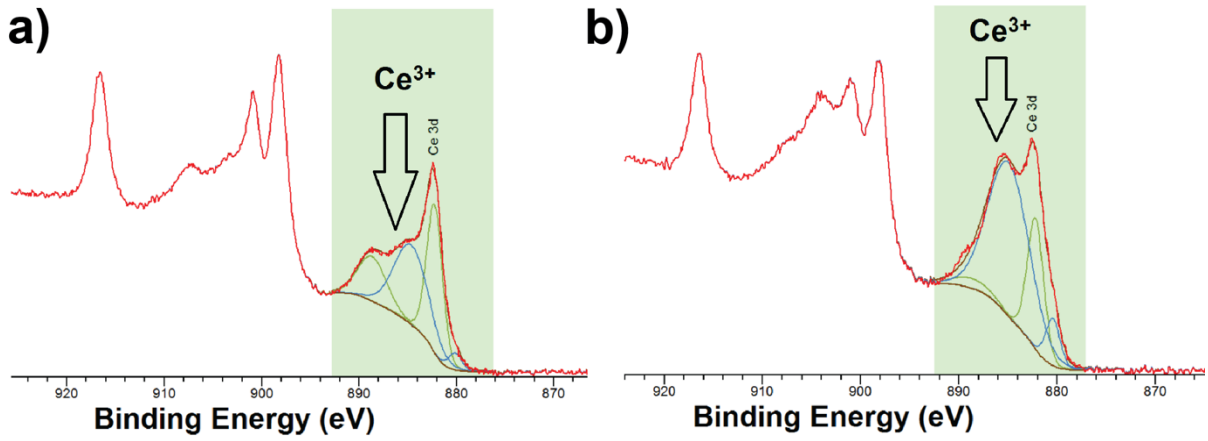

Supplementary Fig 7. Ce 3d spectra of $Mn_{0.30}Ce_{0.19}Ti_{0.51}$ as a) fresh and b) upon SO_2 deactivation.

References

1. Karadağ, H. G.; Bozbağ, S. E.; Şanli, D.; Demir, O.; Ozener, B.; Hisar, G.; Erkey, C., Chapter 4.3 - Mass Transfer Effects in SCR Reactor for NOx Abatement in Diesel Engines. In *Exergetic, Energetic and Environmental Dimensions*, Dincer, I.; Colpan, C. O.; Kizilkan, O., Eds. Academic Press: 2018; pp 961-979.
2. Moulijn, J. A.; Tarfaoui, A.; Kapteijn, F., General aspects of catalyst testing. *Catal. Today* **1991,** *11* (1), 1-12.
3. Bozbağ, S. E., Kinetic model comparison and elucidation of mass transfer limitations in NH3-SCR reactors using Vanadia based washcoats with different thicknesses. *Chem. Eng. Sci.* **2021,** *246*, 116892.
4. Gevers, L. E.; Enakonda, L. R.; Shahid, A.; Ould-Chikh, S.; Silva, C. I. Q.; Paalanen, P. P.; Aguilar-Tapia, A.; Hazemann, J.-L.; Hedhili, M. N.; Wen, F.; Ruiz-Martínez, J., Unraveling the structure and role of Mn and Ce for NOx reduction in application-relevant catalysts. *Nat. Commun.* **2022,** *13* (1), 2960.